

## Hydrogen Peroxide Synthesis

# Safe Direct Synthesis of High Purity H<sub>2</sub>O<sub>2</sub> through a H<sub>2</sub>/O<sub>2</sub> Plasma Reaction\*\*

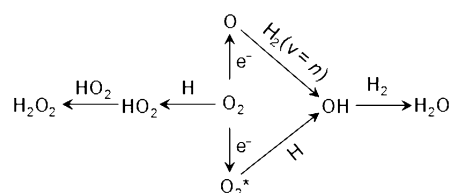
Yanhui Yi, Juncheng Zhou, Hongchen Guo,\* Jianli Zhao, Ji Su, Li Wang, Xiangsheng Wang, and Weimin Gong

Hydrogen peroxide (H<sub>2</sub>O<sub>2</sub>), the most desired green oxidant,<sup>[1]</sup> is almost exclusively produced by an anthraquinone (AQ) process.<sup>[2]</sup> Direct oxidation of H<sub>2</sub> with O<sub>2</sub> has long been considered an ideal alternative for H<sub>2</sub>O<sub>2</sub> production.<sup>[3]</sup> Extensive studies have been done on direct H<sub>2</sub>O<sub>2</sub> synthesis from a H<sub>2</sub>/O<sub>2</sub> mixture. To achieve high efficiency, direct H<sub>2</sub>O<sub>2</sub> synthesis is generally performed in acidified solvent over supported noble-metal catalysts (Au, Pd, Au–Pd, and Pd–Pt).<sup>[4–11]</sup> However, the direct synthesis of H<sub>2</sub>O<sub>2</sub> from a H<sub>2</sub>/O<sub>2</sub> mixture catalyzed by metals is quite hazardous, and it is very difficult to directly obtain high-purity and high-concentration H<sub>2</sub>O<sub>2</sub>.

Research<sup>[12,13]</sup> published in the 1960s has demonstrated that H<sub>2</sub>O<sub>2</sub> can be generated in H<sub>2</sub>/O<sub>2</sub> non-equilibrium plasma through free-radical reactions in the absence of any catalyst or chemical. However, this plasma method has not yet drawn much attention, owing to low H<sub>2</sub>O<sub>2</sub> yield (less than ca. 5 %) and safety concerns about the discharge-triggered H<sub>2</sub>/O<sub>2</sub> reaction.<sup>[12,14]</sup> The content of O<sub>2</sub> must be strictly controlled below 4 mol % in order to prevent explosion and ignition.<sup>[15]</sup>

Our previous research<sup>[16]</sup> showed that the structure of the plasma reactor played an important role in the direct synthesis of H<sub>2</sub>O<sub>2</sub>. A H<sub>2</sub>/O<sub>2</sub> mixture containing 3 mol % of O<sub>2</sub> reaches 100 % O<sub>2</sub> conversion, but the H<sub>2</sub>O<sub>2</sub> selectivity is only 3.5 % (based on O<sub>2</sub>) in a single dielectric barrier discharge (SDBD) plasma reactor with a naked metal high-voltage (HV) electrode and an aqueous grounding electrode. On the other hand, 57.8 % O<sub>2</sub> conversion and 56.3 % H<sub>2</sub>O<sub>2</sub> selectivity (based on O<sub>2</sub>) can be obtained by using a double dielectric barrier discharge (DDBD) plasma reactor with a pyrex-covered metal HV electrode (the pyrex cover acts as an additional dielectric barrier) and an aqueous grounding electrode. Although the selectivity has been greatly improved, the safety concerns and low efficiency, owing to low O<sub>2</sub> content, are still big challenges.

Herein, we report an experimental realization of controllable H<sub>2</sub>/O<sub>2</sub> combustion processes by an optimized plasma reactor. High purity (Grade 1 electronic grade H<sub>2</sub>O<sub>2</sub> according to the SEMI standard) and highly concentrated H<sub>2</sub>O<sub>2</sub> solution (ca. 60 wt %) can be directly produced from a H<sub>2</sub>/O<sub>2</sub> mixture without explosion. These results suggest a different mechanism from conventional H<sub>2</sub>/O<sub>2</sub> combustion processes in the H<sub>2</sub>/O<sub>2</sub> plasma reaction. As shown in Scheme 1, the electron activation of H<sub>2</sub> into H is responsible for H<sub>2</sub>O<sub>2</sub>



**Scheme 1.** Main reaction network for formation of H<sub>2</sub>O<sub>2</sub> and H<sub>2</sub>O in non-equilibrium H<sub>2</sub>/O<sub>2</sub> plasma.

formation. However, the electron activation of O<sub>2</sub> into O and O<sub>2</sub>\* (vibrational and electronic excited states) leads to H<sub>2</sub>O formation and explosion of the H<sub>2</sub>/O<sub>2</sub> mixture. Moreover, low-electron-density H<sub>2</sub>/O<sub>2</sub> plasma leads to a low degree of H<sub>2</sub> and O<sub>2</sub> activation, which plays quite a significant role in producing H<sub>2</sub>O<sub>2</sub> and controlling H<sub>2</sub>/O<sub>2</sub> combustion.

The plasma reactor used in our experiments is a double aqueous electrode DDBD reactor (Supporting Information, Figure S1), which has an aqueous grounding electrode and an aqueous HV electrode. When a mixture of H<sub>2</sub>/O<sub>2</sub> is transformed into H<sub>2</sub>/O<sub>2</sub> plasma, H<sub>2</sub>O<sub>2</sub> and H<sub>2</sub>O are formed and condense on the reactor wall, then flow into the collector.

As shown in Table 1, using the DDBD reactor with double aqueous electrode, the selectivity and concentration of H<sub>2</sub>O<sub>2</sub> are almost more than 60 %. The content of O<sub>2</sub> in the feed can be increased by decreasing the flow rate of H<sub>2</sub>; by this method, the allowable O<sub>2</sub> content reaches 30 mol % while ensuring the safety of the reaction. With a H<sub>2</sub>/O<sub>2</sub> mixture containing 2.0 mol % O<sub>2</sub> at a total flow rate of 500 mL min<sup>−1</sup>, 57 % O<sub>2</sub> conversion and 72 % H<sub>2</sub>O<sub>2</sub> selectivity can be obtained (based on O<sub>2</sub>). The concentration of H<sub>2</sub>O<sub>2</sub> is 67 wt % when the space-time yield of H<sub>2</sub>O<sub>2</sub> is 26 g<sub>H<sub>2</sub>O<sub>2</sub></sub> L<sup>−1</sup> h<sup>−1</sup>. As the content of O<sub>2</sub> in the feed was increased to 14.3 mol %, the conversion of O<sub>2</sub> reached 91 %, and the selectivity and concentration of H<sub>2</sub>O<sub>2</sub> were 64 % and 62 wt %, respectively. In addition, the space-time yield of H<sub>2</sub>O<sub>2</sub> increased to 37 g<sub>H<sub>2</sub>O<sub>2</sub></sub> L<sup>−1</sup> h<sup>−1</sup>.

[\*] Y. H. Yi,<sup>[†]</sup> J. C. Zhou,<sup>[†]</sup> Prof. H. Guo, J. L. Zhao, J. Su, L. Wang, X. S. Wang, W. M. Gong  
State Key Laboratory of Fine Chemicals, Department of Catalytic Chemistry and Engineering Dalian University of Technology  
Dalian 116012 (P.R. China)  
E-mail: hongchenguo@163.com

[†] These authors contributed equally to this work.

[\*\*] We acknowledge the financial support from the Natural Science Foundation of China (20233050). We acknowledge some equipment help from Prof. Ma Xuehu and Prof. Zhang Jialiang.

Supporting information for this article is available on the WWW under <http://dx.doi.org/10.1002/anie.201304134>.

**Table 1:** H<sub>2</sub>O<sub>2</sub> synthesis with varying O<sub>2</sub> content in the double aqueous electrode DDBD reactor.<sup>[a]</sup>

| O <sub>2</sub> content [V %] | O <sub>2</sub> conv. [%] | H <sub>2</sub> O <sub>2</sub> selectivity [%] | C <sub>H<sub>2</sub>O<sub>2</sub></sub> [wt %] | Space-time yield [g <sub>H<sub>2</sub>O<sub>2</sub></sub> L <sup>-1</sup> h <sup>-1</sup> ] <sup>[b]</sup> | Energy consumption [kWh Kg <sub>H<sub>2</sub>O<sub>2</sub></sub> <sup>-1</sup> ] |
|------------------------------|--------------------------|---|--|--|--|
| 2.0                          | 57                       | 72  | 67   | 26   | 27   |
| 4.0                          | 70                       | 70  | 66   | 32   | 23   |
| 6.3                          | 79                       | 68  | 64   | 35   | 20   |
| 9.1                          | 85                       | 66  | 63   | 36   | 20   |
| 14.3                         | 91                       | 64  | 62   | 37   | 19   |
| 20.0                         | 96                       | 59  | 57   | 37   | 19   |
| 25.0                         | 98                       | 57  | 54   | 36   | 20   |
| 30.0                         | 99                       | 50  | 48   | 32   | 22   |

[a] Aqueous grounding electrode at 5 °C, 1 atm, 10 mL min<sup>-1</sup> O<sub>2</sub> flow, input power = 10 W, 14.1 mL reactor. [b] The space-time yield of H<sub>2</sub>O<sub>2</sub> is counted based on 100 wt %. Experimental error: Conversion ± 1 %, Selectivity ± 1 %, C<sub>H<sub>2</sub>O<sub>2</sub></sub> ± 1 wt %, Space-time yield ± 1 g<sub>H<sub>2</sub>O<sub>2</sub></sub> L<sup>-1</sup> h<sup>-1</sup>, Energy consumption ± 1 g<sub>H<sub>2</sub>O<sub>2</sub></sub> kW<sup>-1</sup> h<sup>-1</sup>.

Significantly, without any concentration or purification, the H<sub>2</sub>O<sub>2</sub> solution is obtained in a concentrated (ca. 60 wt %) form, which complies with the requirements for Grade 1 electronic-grade H<sub>2</sub>O<sub>2</sub>, according to the SEMI standard (Table S1).<sup>[17]</sup> The energy consumption for H<sub>2</sub>O<sub>2</sub> production is 19.0 kWh Kg<sub>H<sub>2</sub>O<sub>2</sub></sub><sup>-1</sup> at 14.3 % O<sub>2</sub> (Table 1), which is about a factor of five times higher than for the AQ process. However, the highly energy-consuming concentration and purification processes are avoided, and the equipment investment costs would be dramatically reduced. Therefore, this simple plasma method is attractive for the direct production of concentrated, neutral, and high purity H<sub>2</sub>O<sub>2</sub>, although the selectivity of H<sub>2</sub>O<sub>2</sub> is lower than in AQ process.

Safety is a challenge in the direct synthesis of H<sub>2</sub>O<sub>2</sub> by a H<sub>2</sub>/O<sub>2</sub> mixture because of the broad composition range that is explosive (6–96 mol % O<sub>2</sub>). In the double aqueous electrode DDBD reactor, the H<sub>2</sub>/O<sub>2</sub> plasma reaction is safe when the O<sub>2</sub> content is up to 30 mol %. This is in contrast to a SDBD plasma reactor (Figure S2), where explosions would take place immediately after the start of the discharge when the O<sub>2</sub> content was above 10 mol %. To understand why the H<sub>2</sub>/O<sub>2</sub> plasma reactions can be safely conducted with such a high O<sub>2</sub> content in the double aqueous electrode DDBD reactor, several comparative in situ diagnostic studies were carried out in the SDBD and double aqueous electrode DDBD reactors.

First, the discharge behavior of the double aqueous electrode DDBD reactor is quite different from that of the SDBD reactor. Briefly, the discharge of the SDBD reactor is from spark filaments (local and highly ionized narrow current pathways; Figure 1 a); it is accompanied by strong discharge current pulses (Figure S3) and continuous temperature pulsating (25–50 °C; Figure S4). However, the discharge of the double aqueous electrode DDBD reactor is diffusive and uninterrupted throughout the discharge zone (Figure 1 b); it has weak discharge current pulses (Figure S3) and almost unchanged space temperature (ca. 22 °C; Figure S4C). The higher the discharge current, the higher the electron density. These facts suggest that the reaction temperatures in the two reactors are at a low level and the double aqueous electrode

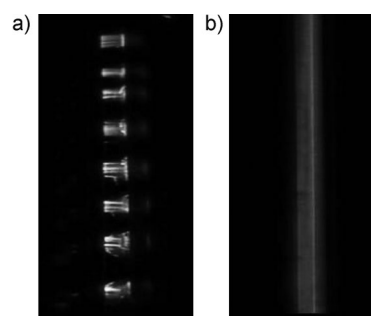


**Figure 1.** Optical images of H<sub>2</sub>/O<sub>2</sub> DBD plasma. a) Optical image in the SDBD reactor. b) Optical image in the double aqueous electrode DDBD reactor. (H<sub>2</sub> 152 mL min<sup>-1</sup>, O<sub>2</sub> 8 mL min<sup>-1</sup>, aqueous grounding electrode at 5 °C, input power 10 W).

DDBD reactor conducts a weak and homogeneous discharge, which has lower electron density.

Second, when the reactors were used for O<sub>2</sub> discharge, optical emission spectra (OES) show that the plasma generated by the SDBD reactor have more intensive O lines (Figure 2 a) and singlet O<sub>2</sub> spectra (Figure 2 b) than the double aqueous electrode DDBD reactor. Similarly, when the reactors were used to synthesize H<sub>2</sub>O<sub>2</sub> through a H<sub>2</sub>/O<sub>2</sub> mixture discharge (Figure 2 c), the plasma generated by the SDBD reactor shows much stronger H lines, O lines and H<sub>2</sub> emission bands than those in the double aqueous electrode DDBD reactor. The intensities of the O lines (777.5 nm and 844.7 nm) increases with increasing O<sub>2</sub> content in both reactors (Figure 2 d; see also Figures S5 A and B), whereas the intensity of the H line shows the reverse trend (Figure S5 C). Surprisingly, when an explosion took place in the SDBD reactor and the double aqueous electrode DDBD reactor, the intensities of the O lines (777.5 and 844.7 nm) were near 260 and 150, respectively; the O<sub>2</sub> content was about 10 mol % for the SDBD reactor and 30 mol % for the double aqueous electrode DDBD reactor. The intensities of the O lines are an indicator of the densities of active oxygen (Sections S7 and S8),<sup>[18]</sup> thus the explosion of H<sub>2</sub>/O<sub>2</sub> mixture under non-equilibrium plasma conditions will take place when the density of active oxygen is beyond the critical value. Moreover, the active oxygen also leads to H<sub>2</sub>O formation.

It seems puzzling that the yields of H<sub>2</sub>O<sub>2</sub> remains at high values for the double aqueous electrode DDBD reactor when the content of O<sub>2</sub> increases from 6.3 % to 30 % (Table 1), as the amounts of O and excited O<sub>2</sub> increase with increasing O<sub>2</sub> content (Figure 2). However, in terms of the relative intensities of the O lines and the degree of activation of O<sub>2</sub>, these values remain constant over the whole range of O<sub>2</sub> content (Figure S7 A and B). Furthermore, the degree of activation of O<sub>2</sub> in the double aqueous electrode DDBD reactor is approximately one third of that in the SDBD reactor. Hence, it is reasonable that the degree of activation of O<sub>2</sub> mainly determines the formation efficiency of H<sub>2</sub>O<sub>2</sub> when the degree of activation of H<sub>2</sub> (Figure S7 C and D) is fixed and sufficient. A low degree of activation of O<sub>2</sub> enhances the formation efficiency of H<sub>2</sub>O<sub>2</sub>, whereas a high degree of activation of O<sub>2</sub> favors the formation of H<sub>2</sub>O. The densities of

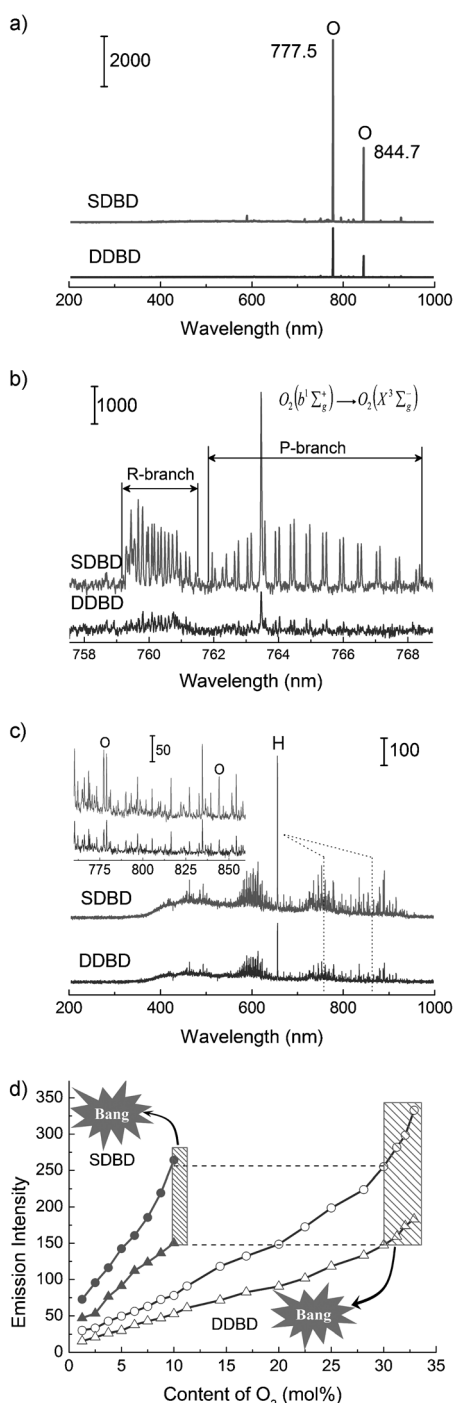


**Figure 2.** OES of  $O_2$  plasma and  $H_2/O_2$  plasma in the SDBD and double aqueous electrode DDBD reactors (aqueous grounding electrode at 5 °C, 1 atm, input power 10 W). a) 40 mL min<sup>-1</sup>  $O_2$  flow, 300 G mm<sup>-1</sup> grating, 0.5 s exposure time. b) 40 mL min<sup>-1</sup>  $O_2$  flow, 1800 G mm<sup>-1</sup> grating, 120 s exposure time. c) 152 mL min<sup>-1</sup>  $H_2$  flow, 8 mL min<sup>-1</sup>  $O_2$  flow, 300 G mm<sup>-1</sup> grating, 0.5 s exposure time. d) Intensity of O lines of  $H_2/O_2$  plasma in the SDBD and double aqueous electrode DDBD reactors with different  $O_2$  content (160 mL min<sup>-1</sup>  $H_2+O_2$  flow, 300 G mm<sup>-1</sup> grating, 0.5 s exposure time). DDBD-O 777.5 nm (○), DDBD-O 844.7 nm (△), SDBD-O 777.5 nm (●), SDBD-O 844.7 nm (▲).

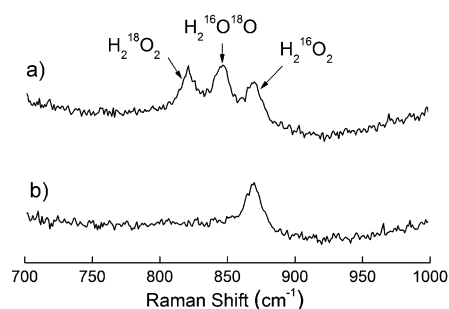


**Figure 3.** Isotopic product distribution of  $H_2O_2$  synthesized by  $H_2/O_2$  plasma. a) 165 mL min<sup>-1</sup>  $H_2$  flow, 4 mL min<sup>-1</sup>  $^{16}O_2$  flow, 4 mL min<sup>-1</sup>  $^{18}O_2$  flow. b) 165 mL min<sup>-1</sup>  $H_2$  flow, 8 mL min<sup>-1</sup>  $^{16}O_2$  flow.

O and excited state  $O_2$  determine whether the explosion of  $H_2/O_2$  takes place.

Third, to understand the mechanism of this  $H_2O_2$  synthesis method, isotope tracing experiments were conducted. Figure 3 shows that the isotopic product distribution of the plasma method is remarkably different from that of the noble-metal-based direct synthesis.<sup>[19]</sup> It can be deduced that the recombination of  $HO_2$  is the primary path of  $H_2O_2$  formation ( $HO_2 + HO_2 \rightarrow H_2O_2 + O_2$ ; Table S2) and  $HO_2$  radical is a key intermediate. This conclusion is consistent with the experimental results. On the one hand, OES analysis (Figure 2c) shows that hydrogen atoms are the main active atom species, which means that  $HO_2$  can be formed by  $H + O_2 \rightarrow HO_2$ . On the other hand,  $H_2O_2$  is the principal product in the double aqueous electrode DDBD reactor. However, the isotope tracing experiments provide little insight into the formation of  $H_2O$ .

Generally, the chain-termination reaction ( $H + O_2 \rightarrow HO_2$ ) leads to  $H_2O_2$  formation, whereas the chain-branching reactions ( $H + O_2 \rightarrow OH + O$  and  $O + H_2 \rightarrow OH + H$ ) result in  $H_2O$  formation.<sup>[20,21]</sup> At ambient temperature, the rate coefficient of the chain termination reaction,  $H + O_2 \rightarrow HO_2$ , is about eight orders of magnitude larger than that of the chain branching reaction,  $H + O_2 \rightarrow OH + O$ , owing to the energy barrier of the latter reaction.<sup>[22,23]</sup> However, the rate coefficient of  $H + O_2 \rightarrow OH + O$  will dramatically increase when the oxygen molecule is in an excited state, because the barriers of the reaction decrease for excited-state  $O_2$ .<sup>[24,25]</sup> Hence, the rate ratio of  $H + O_2 \rightarrow OH + O$  to  $H + O_2 \rightarrow HO_2$  increases with an increase of the ratio of excited  $O_2$  molecules to ground-state  $O_2$  molecules, which results in an increase in the  $OH/HO_2$  ratio. Furthermore,  $OH$  can also be produced by  $O + H_2 \rightarrow OH + H$ , and the O atoms are mainly produced by the electron impact dissociation of  $O_2$  and  $H + O_2^* \rightarrow OH + O$ . The rate coefficient of  $O + H_2 \rightarrow OH + H$  is small, but it can be remarkably enhanced by vibrational excited electronic ground-state  $H_2$ .<sup>[26]</sup> The high concentration of vibrational  $H_2$  in the  $H_2/O_2$  plasma makes this path important for  $OH$  formation (Scheme 1).

It is easy for an explosion to take place in the SDBD reactor. This is because the high electron density results in a high density of  $H_2$  ( $v=n$ ) and active oxygen species (Figure 2), which favors chain-branching reactions (Scheme 1). In the double aqueous electrode DDBD reactor,

the discharge (Figure 1b) is very similar to the Townsend discharges characterized by low current density and low electron density,<sup>[27]</sup> which favors the chain termination reaction and thus results in a low degree of activation of oxygen (Section S9, Figure S7B and D), enhanced safety of the H<sub>2</sub>/O<sub>2</sub> discharge, and the higher selectivity for H<sub>2</sub>O<sub>2</sub> (Scheme 1).

In summary, gaseous H<sub>2</sub>/O<sub>2</sub> plasma reactions have been demonstrated to be controllable for the direct synthesis of H<sub>2</sub>O<sub>2</sub> when using a double aqueous electrode DDBD reactor. In this method, low electron density favors the generation of H<sub>2</sub>O<sub>2</sub> by a chain termination path. This plasma method is promising for the direct synthesis of neutral, high concentration (ca. 60 wt %) and high purity (electronic grade) H<sub>2</sub>O<sub>2</sub>. It has also been successfully integrated with a titanium silicate molecular sieve catalyst for propene epoxidation.<sup>[28]</sup>

On the other hand, the selectivity of H<sub>2</sub>O<sub>2</sub> should be improved further, because it is still much lower than that of the AQ process (above 95%); moreover, more energy efficient means of triggering the H<sub>2</sub>/O<sub>2</sub> plasma reaction should be studied in the future. Significantly, the mechanism of the control process sheds new light on plasma chemistry,<sup>[29]</sup> radical chemistry,<sup>[30,31]</sup> and material treatment by plasma.<sup>[32]</sup> This control process could be helpful for other chemical reactions, especially for certain selective redox reactions.

## Experimental Section

The flow velocities of H<sub>2</sub> and O<sub>2</sub> were monitored by a mass flow controller and mixed homogeneously to pass through the plasma reactor. The temperature of circulating water was maintained at ca. 5°C by a refrigeration unit. After about 10 min (remove O<sub>2</sub> and N<sub>2</sub> to ensure safety), the voltage of the HV electrode was adjusted by controlling the plasma power (high performance computerized plasma and corona discharge experiment generators CTP-2000K) to initiate the DBD discharge. The H<sub>2</sub>/O<sub>2</sub> composition of the feed and effluent was analyzed by an on-line gas chromatograph. The H<sub>2</sub>O<sub>2</sub> concentration of the collected product solution was determined by iodometry, then the H<sub>2</sub>O<sub>2</sub> selectivity was calculated. In the process, the discharge voltage, discharge current, and power were measured on site by a digital oscilloscope (Tektronix DPO 3012, HV probe Tektronix P6015A, current probe Pearson 6585). The discharge images were taken by a camera (Nikon D50).

Received: May 14, 2013

Published online: June 26, 2013

**Keywords:** green chemistry · hydrogen peroxide · plasma chemistry · radical chemistry · synthetic methods

- [1] H. T. Hess in *Kirk-Othmer Encyclopedia of Chemical Engineering* (Eds.: I. Kroschwitz, M. Howe-Grant), Wiley, New York, **1995**, chap. 13, pp. 961.
- [2] J. M. Campos-Martin, G. Blanco-Brieva, J. L. G. Fierro, *Angew. Chem.* **2006**, 118, 7116–7139; *Angew. Chem. Int. Ed.* **2006**, 45, 6962–6984.

- [3] a) V. R. Choudhary, A. G. Gaikwad, S. D. Sansare, *Angew. Chem.* **2001**, 113, 1826–1829; *Angew. Chem. Int. Ed.* **2001**, 40, 1776–1779; b) P. Landon, P. J. Collier, A. J. Papworth, C. J. Kiely, G. J. Hutchings, *Chem. Commun.* **2002**, 2058–2059.
- [4] G. Blanco-Brieva, E. Cano-Serrano, J. M. Campos-Martin, J. L. G. Fierro, *Chem. Commun.* **2004**, 1184–1185.
- [5] a) V. R. Choudhary, C. Samanta, A. G. Gaikwad, *Chem. Commun.* **2004**, 2054–2055; b) V. R. Choudhary, C. Samanta, P. Jana, *Chem. Commun.* **2005**, 5399–5401.
- [6] F. Menegazzo et al., *J. Catal.* **2008**, 257, 369–381.
- [7] a) Q. S. Liu, J. C. Bauer, R. E. Schaak, J. H. Lunsford, *Angew. Chem.* **2008**, 120, 6317–6320; *Angew. Chem. Int. Ed.* **2008**, 47, 6221–6224; b) J. K. Edwards, E. Ntainjua N, A. F. Carley, A. A. Herzing, C. J. Kiely, G. J. Hutchings, *Angew. Chem.* **2009**, 121, 8664–8667; *Angew. Chem. Int. Ed.* **2009**, 48, 8512–8515.
- [8] J. K. Edwards, B. Solsona, E. Ntainjua N, A. F. Carley, A. A. Herzing, C. J. Kiely, G. J. Hutchings, *Science* **2009**, 323, 1037–1041.
- [9] E. N. Ntainjua N, M. Piccinini, S. J. Freakley, J. C. Pritchard, J. K. Edwards, A. F. Carley, G. J. Hutchings, *Green Chem.* **2012**, 14, 170–181.
- [10] a) S. Parasher, M. A. Rueter, B. Zhou, U.S. Patent 20120020872A1, **2012**; b) J. K. Edwards, J. Pritchard, M. Piccinini, G. Shaw, Q. He, A. F. Carley, C. J. Kiely, G. J. Hutchings, *J. Catal.* **2012**, 292, 227–238.
- [11] J. Xu, L. Ouyang, G. J. Da, Q. Q. Song, X. J. Yang, Y. F. Han, *J. Catal.* **2012**, 285, 74–82.
- [12] K. Morinaga, *Bull. Chem. Soc. Jpn.* **1962**, 35, 345–348.
- [13] M. Venugopalan, R. A. Jones, *Chem. Rev.* **1966**, 66, 133–160.
- [14] K. Morinaga, *Bull. Chem. Soc. Jpn.* **1962**, 35, 627–630.
- [15] S. Endoh, K. Namba, S. Yagi, K. Maeda, U.S. Patent 5378436, **1995**.
- [16] J. C. Zhou, H. C. Guo, X. S. Wang, M. X. Guo, J. L. Zhao, L. X. Chen, W. M. Gong, *Chem. Commun.* **2005**, 1631–1633.
- [17] R. Abejón, A. Garea, A. Irabien, *AIChE J.* **2012**, 58, 3718–3730.
- [18] a) R. E. Walkup, K. L. Saenger, G. S. Selwyn, *J. Chem. Phys.* **1986**, 84, 2668–2674; b) M. A. Worsley, S. F. Bent, N. C. M. Fuller, T. Dalton, *J. Appl. Phys.* **2006**, 100, 083301.
- [19] D. P. Dissanayake, J. H. Lunsford, *J. Catal.* **2003**, 214, 113–120.
- [20] E. P. Dougherty, H. Rabitz, *J. Chem. Phys.* **1980**, 72, 6571–6586.
- [21] J. Li, Z. W. Zhao, A. Kazakov, F. L. Dryer, *Int. J. Chem. Kinet.* **2004**, 36, 566–575.
- [22] C. Xu, D. Xie, D. H. Zhang, S. Y. Lin, H. Guo, *J. Chem. Phys.* **2005**, 122, 244305.
- [23] S. R. Sellevåg, Y. Georgievskii, J. A. Miller, *J. Phys. Chem. A* **2008**, 112, 5085–5095.
- [24] J. Y. Ma, H. Guo, C. J. Xie, A. Y. Li, D. Q. Xie, *Phys. Chem. Chem. Phys.* **2011**, 13, 8407–8413.
- [25] G. Quéméner, B. K. Kendrick, N. Balakrishnan, *J. Chem. Phys.* **2010**, 132, 014302.
- [26] R. A. Sultanov, N. Balakrishnan, *Astrophys. J.* **2005**, 629, 305–310.
- [27] U. Kogelschatz, *IEEE. T. Plasma. Sci.* **2002**, 30, 1400–1408.
- [28] J. L. Zhao, J. C. Zhou, J. Su, H. C. Guo, X. S. Wang, W. M. Gong, *AIChE J.* **2007**, 53, 3204–3209.
- [29] W. Sun, M. Uddi, S. H. Won, T. Ombrello, C. Carter, Y. Ju, *Combust. Flame* **2012**, 159, 221–229.
- [30] J. Mao et al., *Atmos. Chem. Phys.* **2010**, 10, 5823–5838.
- [31] P. S. Monks, *Chem. Soc. Rev.* **2005**, 34, 376–395.
- [32] F. S. Denes, S. Manolache, *Prog. Polym. Sci.* **2004**, 29, 815–885.